

Suggested Method for Estimating Maximum Capacity of Images for Different Intensities

Thekra Abbas¹, Zou Beiji² and Ongalo P.N.Fedha³

^{1,2,3} School of Information Science and Engineering , Central South University,
Changsha, 410083, China

Abstract

Digital watermarking has been proposed as a viable solution to the need of copyright protection and authentication of multimedia data in a networked environment, since it makes possible to identify the author, owner, distributor or authorized consumer of a document. Watermarking payload is a topic in which the watermarking researchers have a great interest at present. In this paper, we estimate the maximum watermarking data hiding capacity or the maximum number of bits that can be embedded in spatial domain images under the constraint of perceptual invisibility in the carriers. We studied the maximum payloads under different intensities and verified its effectiveness through experiments

The purpose of the paper, which was to provide a payload reference for watermarking researchers, was achieved by studying the maximum payloads which is related to factors, in addition to the embedding intensity, such as the size of image, image roughness and visual sensitivity.

Keywords: Peak Signal to Noise Ratio(PSNR), Human Visual System(HVS), Mean Square Error(MSE), Visual perceptibility.

1. Introduction

The Information hiding is an emerging research area which encompasses applications such as copyright protection for digital media, watermarking, fingerprinting, steganography, and data embedding.

They share one feature in common: When some data are embedded into the carrier data, no obvious damage is caused. Therefore, the key point of information hiding and digital watermarking is the same [1]. However, differences in their application environments result in different research emphases and requirements. Information hiding emphasizes on the resistance to steganalysis attacks while digital watermarking stresses the perceptual invisibility. In watermarking applications, the message contains information such as owner identification and a digital time stamp. The goal here is usually copyright protection. The message itself is not secret, but it is desired that it permanently resides within the host data set. Similar

requirements exist for systems that embed data (such as object identification, text, or audio), in image and video databases. Such applications are commonly referred to as data hiding or data embedding. In particular, watermarking is now a major activity in audio, image, and video processing.

The existing research literature about information hiding capacity has established theoretical models for information hiding and drawn different capacity expressions for different models. There are some existing methods to estimate the data hiding capacity of digital images [19]–[28]. Most of these methods apply the work of Shannon [7] and Costa [8]. Servetto et al. [19] used statistical models to analyze the robustness of the SST and estimated the watermarking capacity against the jamming noise. Barni et al. [20], [21] modeled each watermark channel by using Generalized Gaussian density to model the full frame DCT coefficients. Moulin and O’Sullivan [2] proposed an information hiding model by abstracting the process of information hiding and using the communication model to represent information hiding. The information hiding capacity is considered as the maximum of reliable transfer rate under the communication model. However, this abstract model is not suitable for the still image information hiding model and cannot be applied to estimate the spatial domain image steganographic capacity. Some papers combined the Information-Theoretic model [1] and perceptual models to estimate the capacity [23], [24]. [25], and [26] focused on comparing the capacity among different transforms such as the identity transform (IT), discrete cosine transform (DCT), Karhunen–Loeve transform (KLT), and the Hadamard transform. Fei et al. [25] suggested that the coefficients in the Slant transform had the highest capacity while Ramkumar et al., [26] indicated that transforms with poor energy compaction property such as Hadamard transform tended to have higher capacity than those with higher energy compaction property such as DCT. Sugihara [27] estimated the capacity by taking robustness of the hidden data into

account. Though the research of Somekh-Baruch and Merhav [4] is an advance for the Moulin model, it is still limited to the communication model. Reference [5] proposed a secure steganographic method based on the payload and analyzed the correlation between image complexity and payload, but this research is confined to the DCT domain and the payload of spatial domain format is not involved. References [6, 7] made an analysis of information hiding capacity by introducing the case theory, but this research can only be made when the carriers follow the Gaussian distribution. At present, most researches focus on how to embed information without visual distortion and there have been few researches on the maximum payload, that is, the maximum payload under the constraint of perceptual invisibility.

In this paper, we attempt to estimate the data hiding capacity on the digital watermarking. To achieve this purpose, this research studies the maximum payloads under different intensities, the watermarking payload estimation method and verifies its effectiveness through experiments. In section 2, we described the watermarking embedding capacity. In section 3 the normalization is explained. The Estimation System of Image Visual Perceptibility described in section 4. Analysis of payload and experimental analysis are explained in section 5 and 6. Section 7 is conclusions and section 8 suggested future works.

2. Watermarking Embedding Capacity

The performance measures to evaluate different data embedding algorithms are the embedding capacity, imperceptibility and robustness. Digital watermarking has a tradeoff between watermark robustness, embedding capacity and image quality. That is, if one of them is increased the other two will be affected. A brief idea of digital watermarking embedding methods is given to understand the influence of embedding intensity on watermarking payload. The traditional image information hiding can be divided into two categories: spatial domain information hiding and frequency domain (DCT, wavelet) information hiding [12].

In spatial domain methods, that our paper belongs to, the watermarking information embeds directly into the cover medium, which involves encoding at the level of the LSBs. Common spatial domain image watermarking formula can be summed up as follows:

$$f_s = f_c + \beta \cdot w \quad \text{or} \quad f_s = f_{c-1} + \beta \cdot w. \quad (1)$$

f_s refers to pixel values of the watermarked image and f_c refers to the clean image, respectively; w and β refers to the secret information embedded and embedding intensity. In the LSB embedding, the value of $\beta \cdot w$ in the first part of formula (1) is -1, 0 or 1. When the value of β is very

large, the embedded information causes great image distortion. Thus, the image quality is changed and embedding fails.

The two types of factors that influence the embedding capacity of the digital image are internal factors and external factors. The external factors are the size of the image and the embedding intensity.

Embedding intensity in data hiding techniques means to embed the secret bit stream from a certain bit plane of the image, and if the secret in bit stream is not finished when this bit plane is full, it can be embedded into the higher bit plane until it is finished.

In our proposed technique the embedding intensity is tested into eight levels, namely, $\beta = 1, 2, \dots, 8$ (Least significant bits). When $\beta = 1$, the embedding begins from the first bit plane line by line. If there is more secret information bit stream to be embedded, it can be embedded into the higher level until it is finished. While $\beta = 2$, the secret information bit stream is embedded from the 2nd bit plane.

Similarly, it is embedded into the higher level until the secret information bit stream is finished. By inference, while $\beta = 8$, the watermark bit stream is embedded into the highest bit plane of the image.

The payload of an image is related to its embedding intensity. Under the constraint of "perceptual invisibility," it is obvious that when $\beta = 1$, the image has the largest payload. The reason why the payloads under different embedding intensities are researched is that when $\beta = 1$, it is actually an LSB watermarking method, for which the current watermarking analysis method is very effective. Under the constraint of perceptual invisibility, there are two factors influencing the payload, image roughness and visual sensitivity.

2.1 Roughness

The maximum payload of an image is closely related to the image itself. The stain can be easily identified in the smooth surface but it is difficult to identify when the surface is rough. Therefore Visual perceptibility of changes in image is not only related to variation but also to roughness of the image.

2.1.2 Texture Roughness Measurement

To measure the texture roughness there are many distribution indicators proposed [21], such as energy, entropy, autocorrelation, covariance, moment of inertia. We employed moment of inertia as the measurement indicator of texture roughness. The formula is as follows:

$$S(r, \theta) = \sum_{a=0}^L \sum_{b=0}^L (a-b)^2 P(a, b) \quad (2)$$

L refers to the highest gray value of the image.

To make the calculation easier, the parameter (r, θ) can be set as specific discrete value, such as $r = 1, 2, 3, \theta = 0, \pi/4, \pi/2, -\pi/4$. When the parameter (r, θ) is set as specific discrete values, the calculation formula for image roughness is

$$Rgh = E(d(r)) = \sum_r a_r d(r) \quad (3)$$

E refers to the mean operator, a_r refers to the weighting factor of moment of inertia $d(r)$ and $\sum_r a_r = 1$. And

$$d(r) = \sum_{\theta} \frac{N(S, \theta)}{N_{\theta}} \quad (4)$$

Figure 1 shows samples images. In the samples image, the roughness of image (b) is the greatest and that of image (d) is the smallest.

2.1.1 2D Histogram

A 2D histogram can be seen as an $M \times N$ matrix, which is called a gray subordinate matrix. For example, take the two pixels $f(i, j)$ and $f(m, n)$ at (i, j) and (m, n) , the distance between the two pixels is r and the line connecting the two points forms an angle of θ with the horizontal line.

If the pixel pairs are highly correlated, then the factors in $Mr, \theta(a, b)$ distribute close to the leading diagonal of the matrix. The approximate estimate of probability distribution of the gray subordinate matrix is

$$P(a, b) \approx \frac{N(a, b)}{M} \quad (5)$$

Where M is the number of image pixels. $N(a, b)$ refers to the number of times that $f(j, k) = a$ and $f(m, n) = b$ appear.

2.2. Visual Sensitivity phenomena

Light is the electromagnetic radiation that stimulates our visual response. There are many factors restricting the perceptibility of human's visual system [23].

2.2.1 Mach Bands Phenomenon

Mach bands phenomenon is an optical illusion, it exaggerates the differences between neighboring areas of slightly differing shades of gray along the boundaries, thus enhancing edge-detection by the human visual system. It is a case in which a target is influenced by its surroundings and produces different perceptions. This phenomenon shows that visual sensitivity is not only influenced by brightness but also by contrast of background. As a result, the perceptibility change caused by information embedding is closely related to these two factors.

Image brightness is a function of shape, reflexes, and illumination [4]. The relationship among them has provided three major research areas in physics-based



Fig. 1 Six images as samples

vision: shape-from-brightness, reflectance-from-brightness, and illumination-from-brightness.

The target brightness of illumination distribution $I(x, y, \lambda)$ is defined as [20, 24] where $V(\lambda)$ is the relative illumination efficiency function of the visual system. To human eyes, $V(\lambda)$ is

$$f(x, y) = \int_0^{\infty} I(x, y) V(\lambda) d\lambda \quad (6)$$

For a grayscale image, its brightness is the pixel value of the image. According to Weber's law, if the brightness f_0 of an object is just noticeably different from the brightness f_s of its surround, then their ratio is

$$\frac{\Delta f}{f} = d(\log f) = \Delta c, \quad (7)$$

In researches on image coding, logarithm law contrast is the widest choice. Logarithm law contrast is defined as follows [20]:

$$Con = 106.3027 \log(f + 1) \quad (8)$$

The eyes are designed to be stimulated by light and to control the amount of light entering the eyeball. The range from scotopic (rod) absolute threshold to a light level that can possibly cause damage covers a luminance range of about 14 log units. Photopic (cone) threshold is almost 4 log units above rod threshold. The sensitivity differences between rods and cones explain the entire 14 log unit range of visual sensitivity. Figure 2 is a simplified homophony visual model.

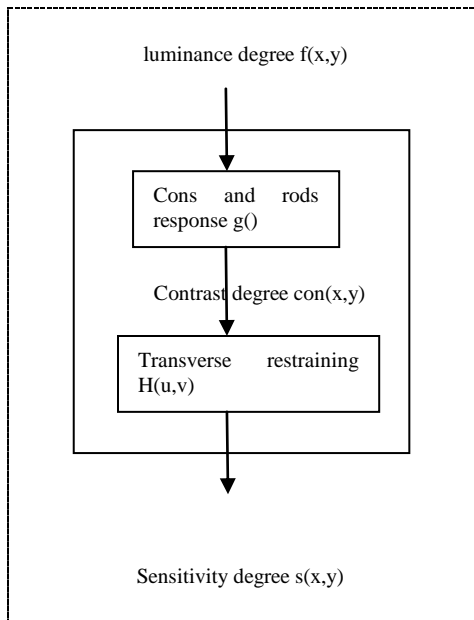


Fig. 2 Simplified homophony visual model nonlinear response of the cone and rod is represented by the point nonlinear function $g(\cdot)$, producing contrast $con(x, y)$.

2.2.2 Lateral Inhibition Phenomenon

Lateral inhibition phenomenon refers to the inhibition that neighboring neurons in brain pathways have on each other. For example, in the visual system, neighboring pathways from the receptors to the optic nerve, which carries information to the visual areas of the brain, show lateral inhibition. This means that neighboring visual neurons respond LESS if they are activated at the same time than if one is activated alone. So the fewer neighboring neurons stimulated, the more strongly a neuron responds. The lateral inhibition phenomenon is represented by a linear system which is spatially invariant and isotropous. Its response frequency is represented by filter $H(u, v)$

$$H(u, v) = H(p) = A \left(\alpha + \left(\frac{p}{p_0} \right)^\gamma \right) \exp \left(- \left(\frac{p}{p_0} \right)^\gamma \right),$$

$$p = \sqrt{u^2 + v^2} \quad (9)$$

where A , α , γ , and p_0 all are constants. p_0 is the peak value frequency while $\alpha = 0$ and $\gamma = 1$. In image processing, it is suitable to choose $A = 2.6$, $\alpha = 0.0192$, $p_0 = 8.772$, and $\gamma = 1.1$. Figure 3 is the response curve of the linear system $H(p)$. From this curve, it can be seen that human eyes have inhibiting effect on low and high frequencies and are most sensitive to changes in medium frequency. From the visual model, the sensitivity $s(x, y)$ can be easily worked out:

$$s(x, y) = \mathfrak{F}^{-1}(con(u, v)H(u, v)),$$

$$con(u, v) = \mathfrak{F}(con(x, y)), \quad (10)$$

where \mathfrak{F} refers to 2D Fourier transform and \mathfrak{F}^{-1} refers to the 2D inverse Fourier transforms. To describe quantitatively the whole sensitivity of human eyes to the single $M \times N$ image, its average value is adopted to represent the image sensitivity ds

$$ds = E(s(x, y)) = \frac{1}{M \times N} \sum_{i=1}^M \sum_{j=1}^N |s(x, y)| \quad (11)$$

the sensitivity values of 6 sample images were listed in the third column in Table 1 Human eyes are most sensitive to changes in sample image (d) but least sensitive to changes in image (e).

From the two sections above we concluded that image roughness is related to visual sensitivity. As shown in figure 3, the visual sensitivity model is not only related to the photo response of cone and rod, but also related to the image contrast which is based on the image content. From the perspective of image roughness, its value is completely dependent on the image content. Thus, image roughness is related to visual sensitivity.

Table 1 Image roughness and visual sensitivity of the sample images

Image	Roughness	Sensitivity
a	120.1	80.348
b	905.51	82.581
c	380.23	86.204
d	671.28	90.310
e	107.956	96.234
f	577.78	88.899

3. Normalization

Normalization is a process that changes the range of pixel intensity values. The linear normalization of a grayscale digital image with intensity values in the range (newMin, newMax). is performed according to the formula

$$I_N = (I - \text{Min}) \frac{\text{newMax} - \text{newMin}}{\text{Max} - \text{Min}} + \text{newMin} \quad (12)$$

Depending on the experiments, image roughness $Rghi$ and visual sensitivity ds_i can be worked out by making use of the image roughness and visual sensitivity, where $i = 1, 2, \dots, 200$ and normalize them according to the formula,

$$N_{rghi} = \frac{Rghi - \min(Rghi)}{\max(rghi) - \min(rghi)}$$

$$N_{ds_i} = \frac{ds_i - \min(ds_i)}{\max(ds_i) - \min(ds_i)} \quad (13)$$

The sensitivity shock is high when the image roughness is small. The sensitivity is stable when the image roughness value is big, and the sensitivity reduces sharply when the

roughness is in the middle. Practically, as the roughness increases as the sensitivity reduces.

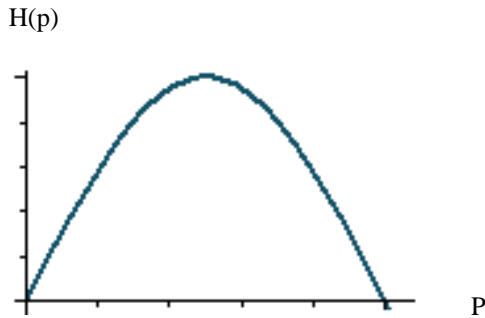


Fig. 3 The response curve of the linear system H(p).

4. The Estimation System of Image Visual Perceptibility

To measure the distortion of the image according to the criteria of digital image processing [12], there are two estimation systems (subjective, objective). In this paper we considered perception rank for the subjective standard and PSNR for the objective standard.

4.1 Perception Rank

Ranks are based on the change rank when an image is compared with an originally (“clean”) image [20]. The image perception changes are rated into five ranks as shown in Table 2.

Several image experts are depended in subjective estimating in watermarking and calculate the average ranks because different individuals have different perceptions and visual sensitivities as represented in the following.

$$R = \left(\frac{\sum_{i=1}^n s_i n_i}{\sum_{i=1}^n n_i} \right) \tag{14}$$

where s_i is the score of rank i , n_i refers to the number of the observers in this gradation, and n refers to the number of ranks.

Figure 4 depicts a subjective decision device, the smaller the value of R is, the lower the perceptibility of the watermarked image is; the larger the value of R is, the

easier the watermarked image is perceived. The change in image R , which the observers cannot judge accurately,

Table 2 Ranks of the images

perception changes	
unnoticeable	-2
not evident	-1
slightly evident	0
evident	1
very evident	2

should be less than -0.1 . Suppose that the observer thinks of a tolerance range as 0.2 , when the average rank R is between $[-0.1, 0.1]$, no judge is made. But when R is larger than 0.1 , the observer can definitely judge that there’s change in perceptibility. This means the embedding fails. Therefore, R of a watermarked image not to be perceived by the observers should be between $[-2, 0.1]$.

4.2 Objective Estimation

Objective estimation is a quantitative measurement, and PSNR is an effective visual fidelity indicator.

PSNR is defined as the ratio of peak signal power to average noise power. Suppose that a watermarked image $f_s(x, y)$ is obtained after a (“clean”) image $f_c(x, y)$ is watermarked, then the mean square error (MSE) σ_e^2 is

$$\sigma_e^2 = E \left[|f_s(x, y) - f_c(x, y)|^2 \right] \tag{15}$$

Then, PSNR using dB as a unit is defined as

$$PSNR = \frac{10 \log_{10}(255 * 255)}{\sigma_e^2} \tag{16}$$

The amount of information is defined as a fixed value $255 * 255$. The variation of the image is only related to the MSE. (The image with a smaller PSNR and a larger MSE can contain more embedding data)

In such a situation, the watermarked image can be perceived more easily. On the contrary, the larger the PSNR and smaller the MSE, less data can be embedded and hence the image is less likely to be perceived. Generally, the change in the image is imperceptible [20] when $PSNR \geq 40$ and when not perceptible when $PSNR < 40$, this is due to it being closely related to the internal factors (mainly the image roughness and visual sensitivity).

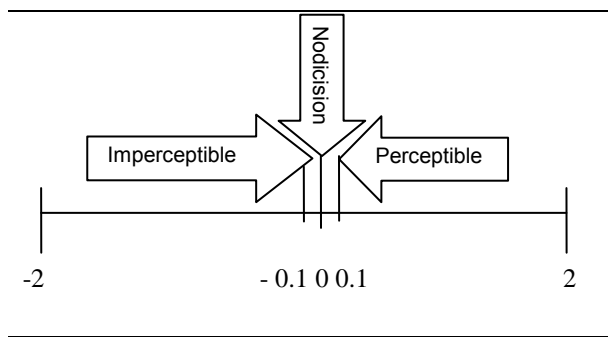


Fig. 4 Discrimination classifier based on subjective estimating.

5. Analysis of Payload

One of the main concerns of the watermarking researchers is the maximum payload of a given image under the constraint of perceptual invisibility. Another concern is the image to be chosen as the carrier to hide a certain amount of watermarking. Both these concerns are related to payload.

The maximum payload of the carrier under a certain constraint is known as maximum payload. It also refers to the higher limit of watermarking data embedded into the image when based on the constraints of “perceptual invisibility”. On exceeding the limit, the image quality is unbearable for the watermarking researchers as it means failure of the watermarking algorithm. This change is then perceived by the observer, that is, the observer discovers this change in the image quality. However, this change can only be discovered when the observer has the original host image. Therefore, it can be concluded that the payload is not only related to the embedding intensity but also to other factors such as visual sensitivity, roughness, size of image and so forth.

5.1. Relation between Payload and Embedding Rate.

For example, a spatial grayscale image $f(x,y)$ with a $M \times N$ to be embedded, and under the constraint of perceptual invisibility, then the arithmetic model for estimating its maximum payload is

$$c_f = size * Re(\beta, Rgh, ds)$$

$$\text{condition: } R \leq 0.1 \quad (17)$$

Here, $size = M * N$, β refers to the embedding intensity, Rgh refers to image roughness, ds refers to visual sensitivity, and the constraint R refers to subjective estimating rank. In most situations, the size of the image is proportional to the payload, for example the larger the size of the image is, the greater the payload, and vice versa.

Suppose that the embedding rate is Re (bits per pixel, bpp). Then, the relation between the embedding rate and embedding intensity, roughness, and sensitivity is

$$Re = \frac{C_f}{size} = Re(\beta, Rgh, ds) \quad (18)$$

In order to obtain the maximum payload of the image, the first thing that should be obtained is the relation between the embedding rate and embedding intensity, roughness and sensitivity.

The next section will analyze the influence of embedding intensity on embedding rate with the objective estimating system.

5.2. Relation between Embedding Rate and Embedding Intensity.

The concept of embedding factor is introduced in order to describe the relation between embedding rate and embedding intensity.

Embedding factor λ refers to embed secret information bit stream only into a single bit plane of the image. For instance, if the secret information bit stream is only embedded into the first bit plane, then $\lambda = 1$ or $\lambda = 2$ if it is only embedded into the second bit plane and so on.

The difference e , which is 0, -1, or 1, only happens on the i th plane and it only happens between watermarked image and clean image when secret information bit stream is embedded into the i th plane.

Its probability to appear is [25]

$$P(e) = \begin{cases} \frac{1}{4}, e = -1, \\ \frac{1}{2}, e = 0, \\ \frac{1}{4}, e = 1 \end{cases} \quad (19)$$

If embed information with the embedding rate of $Re_{\lambda=i}$ into the i th bit plane, its MSE is

$$E(\sigma_e^2 | \lambda = i) = (Re_{\lambda=i}) * \sum_{e=-1}^1 (e * 2^{i-1})^2 * P(e) \quad (20)$$

If it is full embedded on the i th bit plane, that is, when $Re_{\lambda=i} = 1$, the mean square error on this level is

$$A_{er_i} = \sum_{e=-1}^1 (e * 2^{i-1})^2 P(e) \quad (21)$$

Hence, the relation between the embedding rate and the mean square error and on the i th bit place is easier to obtain when it is not fully embedding.

$$Re_{\lambda=i} = \frac{\sigma_e^2}{A_{er_i}} \quad (22)$$

However, as the visual imperceptibility is related to image roughness and visual sensitivity, it is difficult to get the maximum mean square error beforehand. Therefore, subjective estimation (MSE belongs to objective estimation) is used in the next section to deduce the relation between the maximum embedding rate and image roughness and visual sensitivity.

6. Experimental Analysis

The 200 various images that were tested were downloaded from the internet [26]. Images included simple images without any detail and also those containing great details. There are images of rivers, buildings, mountains, faces, and so on. (ACDsee image treatment software was used to treat all images; the colorful ones were transferred into gray ones and cut into size (256 x 256) and the non-BMP images were transferred into BMP ones. Samples of these images are shown in figure 2.

From the experiment, result we obtained that the payload related to the roughness and visual sensitivity in addition to the image size and embedding intensity. So we have discussed the following aspects:

1. The relation between the maximum payload and the image size.
2. The relation between the embedding rate and the embedding intensity.
3. The relationship model of the embedding rate and the image roughness, visual sensitivity by:

a- Increasing the payload dynamically in the process and judged, depending on the observation whether any visual perceptibility has happened. In the proposed scheme we change the embedding intensity β . Given a certain β , the embedding information begins to be embedded from the β th bit plane. Then, continue to embed from level $\beta + 1$, the embedding will not stop until visual perceptibility happens in the image. Figure 5 shows the embedding rates when the embedding intensity $\beta = 1$.

b- Depending on the experiments results, when the embedding intensity is full and it is only embedded into the first bit plane (LSB embedding method), its PSNR is far higher than 40($E(\text{PSNR} | \lambda = 1) = 52.343$), which is to say HVS can hardly perceive the changes in the image. But from the 2nd bit plane, PSNR is lower than the secure value of 40, and the watermarked image may be perceived. When first, second, and third bit plane are all embedded with secret information, its PSNR is 38.412, and then the possibility of its being perceived is greater. It can be concluded that whether the first bit plane is embedded with information or not exerts little influence on visual perceptibility of the image. This is only the possibility of

being detectable, whether it is really perceptible is closely related to image roughness and visual sensitivity.

Our experiment concentrated on calculating maximum embedding rate from level 2, that is, when $\beta = 2$. The experiment plan can be designed as shown in figure 6.

A host image is selected at random. Firstly, the roughness and sensitivity is calculated. Then, the watermarking information is embedded constantly, without causing any visual perceptibility, until perceptual visibility happens to the image. The embedding rate value can be deduced by dividing the embedding amount until the last embedding by the size of the image.

From the above analysis we conclude that under the constraint of perceptual invisibility the key to working out the maximum payload is to work out the maximum embedding rate. In the experiments the following steps followed to embed the information:

Some participants, who had participated in image treatment for a long time, were invited to evaluate the perceptible changes.

a-The information is embedded from the second bit plane.

b-If the second bit plane is full, and the average level mark of the determining team is $R < 0.1$; the information is embedded into the next bit plane

c-If $R \geq 0.1$, the image cannot be embedded with information, and the estimation is over then, the estimation of the next image begins.

d- When $\beta = 2$, the maximum payload for this image is the information altogether until it is embedded into the last level.

From the experiment the relationship model between the embedding rate and image roughness can be suggested as

$$Re_3 = a + b \log_c(1 + d * Rgh) \quad (0 \leq Rgh \leq 1), \quad (23)$$

while the embedding rate and visual sensitivity, in general, show an inverted U shape. As a result, their relationship model can be constituted as

$$Re_4 = e - f * (Sens - 0.6)^2 \quad (0 \leq Sens \leq 1). \quad (24)$$

where a, b, c, e, f and d in formula(23) and (24) are unknown constants. Using these two formulas by geometric mean, and the relation of the surface model between the maximum embedding rate and image roughness when $\beta = 2$. Subsequently, the new formula is

$$Re_{\beta=2} = \sqrt{a + b \log_c(1 + d * Rgh)} * \sqrt{e - f(Sens - 0.6)^2} \quad (25)$$

We calculate the actual embedding rate of the 200 images and the estimated minimum mean square error of the embedding rate in (24), we obtain the values of the unknown constants as follows

$$a = 0.9430, \quad b = 2.5613, \quad c = 101.7520, \quad d = 101.4355, \\ e = 3.6930, \quad f = 9.96500.$$



Fig.5 The sample images with payload of 80.8 k, 141.6 k, 194.8 k bits using our watermark method while $\beta = 1$.

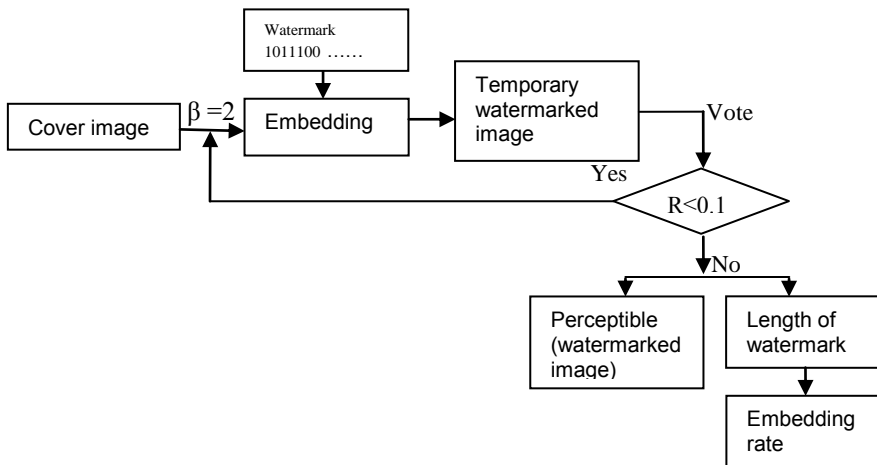


Fig. 6 The block diagram of incremental embedding procedure to determine the embedding rate.

Then we applied formula (25) to calculate the maximum embedding rate of the image when the embedding intensity $\beta = 2$.

On the basis of this maximum embedding rate, to work out the maximum embedding rate under various embedding intensities, the mean square error is used.

When the maximum mean square error σ^2e is obtained, the maximum embedding rate R_e (β , R_{gh} , $Sens$) under various embedding intensities and the maximum payload are calculated by using (17).

6.1 Error Rate Calculation.

To evaluate the effectiveness of the suggested estimation method for maximum embedding capacity error rate is considered as evaluation indicator.

$$R_{error} = \frac{|a-b|}{a} \tag{26}$$

a is the actual maximum capacity of an image, b is the estimated maximum capacity.

In the experiment the actual maximum payload of 200 images under $\beta = 1, 2, 3$ are calculated as shown in Table 3, by the judge experts and the estimated maximum payload using our method. The result satisfied what we discovered above that as the embedding intensity grew larger, the payload became smaller. The error rate in (26) reflects the deviation rate between the image actual payload and the estimated payload. Figure 7 shows the error rate of the payload of the 200 images tested. From Figure 7, it can be seen that the estimation of most images are highly accurate. There is little difference between the actual payload and the estimated payload. But difference between the actual payload and the estimated payload for few images is relatively great, with some approaching 50%. Table 4 shows the mean value and the standard deviation of the 200 images in the experiment.

Table 3: Actual and estimation payload for the six sample images

Actual maximum payload (kilobits)	Sample images	$\beta = 1$	$\beta = 2$	$\beta = 3$
	a		277.90	214.15
b		248.80	185.80	125.80
c		250.42	200.45	140.42
d		185	125	77
e		219.07	156.07	96.07
f		193	143	95
Estimated maximum payload (kilobits)	a	246.25	182.80	121.35
	b	278.25	214.85	153.45
c	276.75	213.35	151.85	
d	217.05	155.50	101.50	
e	269.75	206.50	145.05	
f	235.05	173.50	129.50	

Generally, our estimation method is effective in that the average error rate of images tested under various intensities is less than 15% and the standard deviation is within 13%. From Table 3, it can be concluded that the larger the embedding intensity is, the smaller the difference between the estimated payload and the actual payload is and the higher the accuracy is. The reason is that when the embedding intensity is low, the payload is larger and it is easier for deviation to appear.

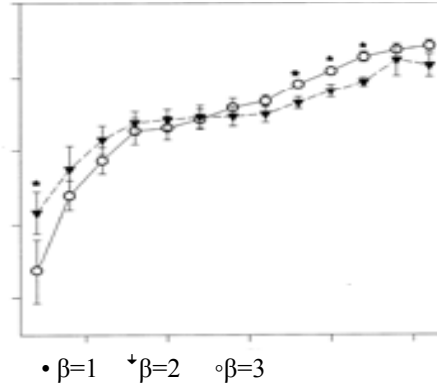


Fig. 7 The error rate of 200 images

The reason is that when the embedding intensity is low, the payload is larger and it is easier for deviation to appear.

Table 4: The mean and standard deviation of 200 image's error rates

Embedding intensity	Mean	Standard deviation
$\beta = 1$	0.139	0.12261
$\beta = 2$	0.13512	0.1171
$\beta = 3$	0.12309	0.10291
Average	0.1324	0.1142

7. Conclusion

The external factors that influenced the maximum payload are mainly the image size, embedding intensity.

The internal factors are mainly the image roughness, visual sensitivity, and so forth.

Higher bits embedding generates more noise than lower bits embedding does (image distortion), therefore the embedding intensity is in inversely proportional to the payload while the size of image is in direct proportion to the payload.

The HVS have variance sensitivity to changes in different images, which are affected by image contrast and brightness.

While it is difficult for the human eyes to identify the subtle changes in a highly rough image, it is easy to identify such changes in a smooth image, therefore different degrees in roughness result in different perceptibility.

While the relationship model between visual sensitivity, watermarking payload and image roughness is deduced through effective experiments designed on the basis of subjective estimating indicators, the correlation between the maximum payload, the embedding intensity and the size of image is theoretically deduced through the objective estimation indicator of the peak signal to noise rate (PSNR).

Acknowledgments

Supported by the National Science Foundation of China under Grant No. 60970098, Modeling for Human Visual System and its application; The National Science Foundation of China under Grant No. 61173122, A Fast Three-dimensional Reconstruction Based on Image by Simulating Mechanisms of Human Visual System.

References

- [1] X. X. Niu and Y. X. Yang, "Study on the frame of information steganography and steganalysis," *Acta Electronica Sinica*, vol. 34, pp. 2421–2424, 2006.
- [2] P. Moulin and J. A. O'Sullivan, "Information-theoretic analysis of information hiding," *IEEE Transactions on Information Theory*, vol. 49, no. 3, pp. 563–593, 2003.
- [3] T. Cover and J. Thomas, *Elements of Information Theory*. New York: Wiley, 1991.
- [4] A. Somekh-Baruch and N. Merhav, "On the capacity game of public watermarking systems," *IEEE Transactions on Information Theory*, vol. 50, no. 3, pp. 511–524, 2004.
- [5] H. Sajedi and M. Jamzad, "Secure steganography based on embedding capacity," *International Journal of Information Security*, vol. 8, no. 6, pp. 433–445, 2009.
- [6] H. Y. Gao, *The theory and application of audio information hiding*, PH.D. dissertation, Beijing University of Posts and Telecommunications, Beijing, China, 2006.
- [7] R. Chandramouli and N. D. Memon, "Steganography capacity: a steganalysis perspective," in *Security and Watermarking of Multimedia Contents*, vol. 5020 of *Proceedings of SPIE*, pp. 173–177, Springer, Santa Claru, Calif, USA, 2003.
- [8] S. Li, X. P. Zhang, and S. Z. Wang, "Digital image steganography based on tolerable error range," *Journal of Image and Graphics*, vol. 12, no. 2, pp. 212–217, 2007.
- [9] D. Kundur, "Implication for high capacity data hiding in the presence of lossy compression," in *Proc. IEEE Int. Conf. Information Technology: Coding and Computing*, Mar. 2000.
- [10] C. Y. Lin and S. F. Chang, "Watermarking capacity of digital images based on domain-specific masking effects," in *Proc. IEEE Int. Conf. Information Technology: Coding and Computing*, Apr. 2001, pp. 90–94.
- [11] X. Zhang and S. Wang, "Steganography using multiple-base notational system and human vision sensitivity," *IEEE Signal Processing Letters*, vol. 12, no. 1, pp. 67–70, 2005.
- [12] C. Fei, D. Kundur, and R. Kwong, "The choice of watermark domain in the presence of compression," in *Proc. IEEE Int. Conf. Information Technology: Coding and Computing*, Apr. 2001, pp. 79–84. [13] M. Ramkumar and A. N. Akansu, "Capacity estimates for data hiding in compressed images," *IEEE Trans. Image Processing*, vol. 10, pp. 1252–1263, Aug. 2001.
- [14] C. Y. Lin and S. F. Chang, "Watermarking capacity of digital images based on domain-specific masking effects," in *Proc. IEEE Int. Conf. Information Technology: Coding and Computing*, Apr. 2001, pp. 90–94.
- [15] R. Sugihara, "Practical capacity of digital watermark as constrained by reliability," in *Proc. IEEE Int. Conf. Information Technology: Coding and Computing*, Apr. 2001.
- [16] C. Fei, D. Kundur, and R. Kwong, "The choice of watermark domain in the presence of compression," in *Proc. IEEE Int. Conf. Information Technology: Coding and Computing*, Apr. 2001, pp. 79–84.
- [17] X. Zhang and S. Wang, "Efficient steganographic embedding by exploiting modification direction," *IEEE Communications Letters*, vol. 10, no. 11, pp. 781–783, 2006.
- [18] Z. G. Qu, Y. Fu, X. Niu, Y. Yang, and R. Zhang, "Improved EMD steganography with great embedding rate and high embedding efficiency," in *Proceedings of the International Conference on Intelligent Information Hiding and Multimedia Signal Processing (IIH-MSP '09)*, Japan, 2009.
- [19] W. N. Lie and G. S. Lin, "A feature-based classification technique for blind image steganalysis," *IEEE Transactions on Multimedia*, vol. 7, no. 6, pp. 1007–1020, 2005.
- [20] A. K. Jain, *Fundamentals of Digital Image Processing*. Person Education, Inc., Publish as Prentice Hall, 1989.
- [21] C. H. Yang, C. Y. Weng, S. J. Wang, and H. M. Sun, "Adaptive data hiding in edge areas of images with spatial LSB domain systems," *IEEE Transactions on Information Forensics and Security*, vol. 3, no. 3, pp. 488–497, 2008.
- [22] B. Benita II M.E. (CSE), PSNCE, "Enhanced Digital Watermarking Algorithm for Directionally Selective and Shift Invariant Analysis" *IJCSI International Journal of Computer Science Issues*, Vol. 8, Issue 1, January 2011.
- [23] J. F. Delaigle, C. Devleeschouwer, B. Macq et al., "Human visual system features enabling watermarking," in *Proceedings of IEEE International Conference on Multimedia and Expo*, pp. 489–492, Switzerland, 2002.
- [24] Abdulaleem Z. Al-Othmani, Azizah Abdul Manaf and Akram M. Zeki "A Survey on Steganography Techniques in Real Time Audio Signals, Evaluation" *IJCSI International Journal of Computer Science Issues*, Vol. 9, No 1, 2012.
- [25] A. D. Ker, "A capacity result for batch steganography," *IEEE Signal Processing Letters*, vol. 14, no. 8, pp. 525–528, 2007.
- [26] <http://images.search.yahoo.com/search/images>

Thekra Abbas BSc in computer science, from University of Technology in Baghdad 1987. MSc in computer science from Al-Mustanseriya University in Baghdad 2005. Since 2009, Eng. now She is studying towards her PhD degree at the School of Information Science and Engineering, Central South University, Changsha, China. She served as Head of the Computer Laboratories in the College of Science in Al-Mustanseriya University from 1997 to 2003. She worked as a lecturer and associate professor in Al-Mustanseriya University, Baghdad, Iraq from 2005 to 2009. Her research interest includes Image processing, Information Hiding.

Prof. Dr. Zou Baiji 1978 – 1982 Zhejiang University, Hangzhou, China BSc Computer Software. 1982 – 1984 Qinghua University, Beijing, China. MSc Computer Application. 1997 – 2001 Hunan University, Changsha, China. Ph.D. Control Theory and Engineering. Research Experience. 2002 – 2003 Qinghua University Post Doctor. 2003 – 2004 Griffith University, Australia. Visiting Scholar. Vice Dean of School of Information Science and Engineering, Central South University, China. His research interest includes Digital image processing, Computer Graphics, Multi-Media Technology and Software Engineering.

Ongalo P.N. Fedha BSc and MSc in computer science from Nairobi University, Kenya in 1998 and 2008. Since 2009, Eng. Now she is studying her PhD degree at the School of Information Science and Engineering, Central South University, Changsha, China.